Atmos. Chem. Phys. Discuss., 15, 33209–33251, 2015
www.atmos-chem-phys-discuss.net/15/33209/2015/
doi:10.5194/acpd-15-33209-2015

Atmospheric Chemistry and Physics Discussions

The impact of monthly variation of the Pacific-North America (PNA) teleconnection pattern on wintertime surface-layer aerosol concentrations in the United States

J. Feng[1,2], **H. Liao**[1], **and J. Li**[3]

[1]State key Laboratory of Atmospheric Boundary Layer Physics and Atmospheric Chemistry, Institute of Atmospheric Physics, Chinese Academy of Sciences, Beijing, China
[2]University of Chinese Academy of Science, Beijing, China
[3]College of Global Change and Earth System Science, Beijing Normal University, Beijing, China

Received: 13 October 2015 – Accepted: 10 November 2015 – Published: 25 November 2015

Correspondence to: H. Liao (hongliao@mail.iap.ac.cn)

Published by Copernicus Publications on behalf of the European Geosciences Union.

Abstract

The Pacific-North America teleconnection (PNA) is the leading general circulation pattern in the troposphere over the region of North Pacific to North America during wintertime. This study examined the impacts of monthly variation of the PNA phase (positive or negative phase) on wintertime surface-layer aerosol concentrations in the US by analyzing observations during 1999–2013 from the Air Quality System of Environmental Protection Agency (EPA-AQS) and the model results for 1986–2006 from the global three-dimensional Goddard Earth Observing System (GEOS) chemical transport model (GEOS-Chem). The composite analyses on the EPA-AQS observations over 1999–2003 showed that the average concentrations of $PM_{2.5}$, sulfate, nitrate, ammonium, organic carbon, and black carbon aerosols over the US were higher in the PNA positive phases than in the PNA negative phases by 1.4 $\mu g\,m^{-3}$ (12.7 %), 0.1 $\mu g\,m^{-3}$ (6.4 %), 0.3 $\mu g\,m^{-3}$ (39.1 %), 0.2 $\mu g\,m^{-3}$ (22.8 %), 0.8 $\mu g\,m^{-3}$ (21.3 %), and 0.2 $\mu g\,m^{-3}$ (34.1 %), respectively. The simulated geographical patterns of the differences in concentrations of all aerosol species between the PNA positive and negative phases were similar to observations. Based on the GEOS-Chem simulation driven by the assimilated meteorological fields, the PNA-induced variation in planetary boundary layer height was found to be the most dominant meteorological factor that influenced the concentrations of $PM_{2.5}$, sulfate, ammonium, organic carbon, and black carbon, and the PNA-induced variation in temperature was the most important parameter that influenced nitrate aerosol. Results from this work have important implications for understanding and prediction of air quality in the United States.

1 Introduction

Aerosols are the major air pollutants that have adverse effects on human health, reduce atmospheric visibility, and influence climate through aerosol-radiation and aerosol-cloud interactions (IPCC, 2013). Aerosol concentrations are high over the industrial-

ACPD
15, 33209–33251, 2015

ized regions such as the US, Europe, and East Asia, which are driven by emissions of aerosols and aerosol precursors (Dutkiewicz et al., 2000; Vestreng et al., 2007; Hand et al., 2012a; Mijling et al., 2013) and regional meteorological conditions.

Previous studies have shown that aerosol concentrations are very sensitive to meteorological parameters (Aw and Kleeman, 2003; Wise and Comrie, 2005; Dawson et al., 2007; Kleeman, 2008; Jacob and Winner, 2009; Tai et al., 2010, 2012a). Aw (2003) examined the sensitivity of $PM_{2.5}$ (aerosol particles which diameter $\leq 2.5\,\mu m$) concentration to temperature by performing sensitivity studies in the California Institute of Technology/UC Davis (CIT/UCD) air quality model. A cross-board increase in temperature by 5 K in Southern California on 25 September 1996, led to decreases in peak $PM_{2.5}$ concentrations by up to $30.7\,\mu g\,m^{-3}$ ($\sim 30\,\%$). Wise and Comrie (2005) reported, by statistical analyses of observational datasets obtained from Air Quality System of US Environmental Protection Agency (EPA-AQS), that the variations in meteorological parameters accounted for 20–50 % of the variability in aerosol levels over 1990–2003 in five metropolitan areas in the southwestern US. They found that aerosols in these five cities were most sensitive to relative humidity. Dawson et al. (2007) found, by sensitivity studies in the Particulate Matter Comprehensive Air Quality Model with extensions (PMCAMx), that $PM_{2.5}$ concentrations in summer had a small sensitivity to temperature increases ($-16\,ng\,m^{-3}\,K^{-1}$ on average) because the increases in sulfate offset the decreases in nitrate and organics, while $PM_{2.5}$ concentrations in winter decreased significantly with temperature ($-170\,ng\,m^{-3}\,K^{-1}$ on average) because the increases in temperature led to large reductions in nitrate and organics. Dawson et al. (2007) also showed that $PM_{2.5}$ concentrations increased with humidity in both winter and summer. Jacob and Winner (2009) summarized by literature review that the regional stagnation, mixing depth, and precipitation are the most important meteorological parameters that influence surface-layer aerosol concentrations. Future climate change was also simulated to influence aerosol levels over the US by about $1\,\mu g\,m^{-3}$ (Jacob and Winner, 2009), as a result of the climate-induced changes in atmospheric oxidants, transport, deposition, and the shift of gas-particle equilibria (Liao et al., 2006; Unger et al., 2006;

ACPD
15, 33209–33251, 2015

Bauer et al., 2007; Jacob and Winner, 2009; Pye et al., 2009; Lam et al., 2011; Day and Pandis, 2011; Juda-Rezler et al., 2012; Tai et al., 2012b).

Previous studies have also reported that the changes in atmospheric circulation pattern, such as the East Asian Summer Monsoon (EASM), North Atlantic Oscillation (NAO), and El Niño-South Oscillation (ENSO), can modulate distributions and concentrations of aerosols. Zhu et al. (2012) found, by simulation of aerosol concentrations over years 1986–2006 with the global chemical transport model GEOS-Chem, that the decadal-scale weakening of the EASM led to increases in aerosol concentrations in eastern China, and summertime surface aerosol concentrations in the weakest EASM years were larger than those in the strongest EASM years by approximately 20 %. Moulin et al. (1997) showed that the variations in NAO could influence mineral dust aerosol transported to the North Atlantic Ocean and the Mediterranean Sea, since the mean aerosol optical depth (AOD) of dust in summer correlated with the NAO index during 1983–1994 with a correlation coefficient of 0.50. Jerez et al. (2013) found, by simulations of aerosols for years 1970–1999 with the CHIMERE chemistry transport model driven by the BCMWF ERA40 reanalysis data, that the concentrations of PM_{10} and $PM_{2.5}$ in the southern European regions in winter differed by 10 and 20 $\mu g\,m^{-3}$, respectively, between the positive and negative NAO phases. By using the multi-angle imaging spectroradiometer satellite (MISR) datasets of AOD during 2000–2011, Liu et al. (2013) found a period of 3–4 years in observed summertime AOD over the North China Plain (NCP), and the peak of summertime AOD in NCP occurred four months later after the rapidly transition of El Niño from a warm phase to a cold phase because of the associated cyclone anomaly and maritime inflow over the NCP. Singh and Palazoglu (2012) found correlations between PDO and ENSO and the aerosol exceedance days (defined as the days with $PM_{2.5}$ concentrations larger than the US National Ambient Air Quality Standard) at 6 regions in the US by using the EPA-AQS $PM_{2.5}$ wintertime datasets during 1950–2008.

The Pacific-North America teleconnection pattern (PNA) is one of the most recognized, influential climate patterns in the mid-latitudes over the region of North Pacific to

ACPD
15, 33209–33251, 2015

North America during wintertime with monthly variations (Wallace and Gutzler, 1981; Blackmon et al., 1984; Liang et al., 2005; Athanasiadis and Ambaum, 2009). The PNA phase is defined by the geopotential height anomalies in the middle troposphere over the vicinity of Hawaii, the south of the Aleutian Islands, the intermountain region of North America, and the Gulf Coast region in the US (Wallace and Gutzler, 1981). A positive (negative) PNA phase is characterized by positive (negative) geopotential height anomalies over the vicinity of Hawaii and the northwestern North America, while negative (positive) geopotential height anomalies over south of the Aleutian Islands and the Gulf Coast region (see Fig. S1 in the Supplement).

The PNA has large impacts on surface-layer meteorological variables in the US during wintertime. Previous studies have reported strong positive (negative) correlation between PNA and surface ambient temperature in the northwestern (southeastern) US (Leathers et al., 1991; Redmond and Koch, 1991), and negative correlation between PNA and precipitation rate (Leathers et al., 1991; Coleman and Rogers, 2003) and moisture (Coleman and Rogers, 2003) in the contiguous Ohio River Valley. These variations in meteorological parameters in the US are associated with the PNA-induced anomalies in jet stream position, activities of cold fronts, and synoptic cyclones (Leathers et al., 1991; Notaro et al., 2006; Myoung and Deng, 2009).

Several studies have examined the impacts of PNA on aerosols. Gong et al. (2006) studied the interannual variations in the trans-Pacific transport of Asian dust during 1960–2003 by using the Northern Aerosol Regional Climate Model (NARCM). They found a negative correlation (with a correlation coefficient of −0.55) between the PNA and the ratio of dust mass that reached the North American continent to that exported from Asia because of the strong westerly jet in the East Pacific during the negative PNA phases. Di Pierro et al. (2011), by using satellite retrieval of aerosol optical depth (AOD) from Cloud-Aerosol Lidar with Orthogonal Polarization (CALIOP), identified 11 events of Asian aerosol transport to the Arctic during 2007 to 2009, in which 4 events were associated with the negative PNA phases. These studies, however, were focused on the impact of PNA on the transport of aerosols due to the variations in westerly jet

ACPD
15, 33209–33251, 2015

stream and blocking activity. Furthermore, these studies were limited to aerosols in the regions of North America and the Arctic.

We examine in this work the impacts of monthly variations in PNA phase on aerosol concentrations in the US during wintertime, by analyses of the observed aerosol concentrations during 1999–2013 from EPA-AQS and also by simulations of aerosol concentrations for years 1986–2006 using the global chemical transport model GEOS-Chem. The scientific goals of this work are (1) to quantify the differences in wintertime concentrations of sulfate (SO_4^{2-}), nitrate (NO_3^-), ammonium (NH_4^+), black carbon (BC), organic carbon (OC), and $PM_{2.5}$ in the US between different PNA phases, and (2) to understand the roles of PNA-induced variations in meteorology (for example, surface air temperature, wind speed, planetary boundary layer height, precipitation, and relative humidity) in influencing the wintertime aerosol concentrations. The descriptions of the PNA index, EPA-AQS observation data, and numerical simulation in the GEOS-Chem model are shown in Sect. 2. Sections 3 and 4 present the impacts of the PNA on wintertime aerosol concentrations in the US obtained from the EPA-AQS observations and the GEOS-Chem simulation, respectively. The mechanisms for the impacts of PNA on aerosols are examined in Sect. 5.

2 Data, simulation, and methodology

2.1 Observed aerosol concentrations

Observed concentrations of aerosols are obtained from the Air Quality System of the US Environmental Protection Agency (EPA-AQS, http://www.epa.gov/airquality/airdata/). The EPA-AQS daily $PM_{2.5}$ mass concentrations are available over 1999–2013 at about 1200 sites, and the speciated aerosol concentrations, including those of SO_4^{2-}, NO_3^-, NH_4^+, BC, and OC, are available for 2000–2013 at about 300 sites.

The measurements of aerosol concentrations from the EPA-AQS were carried out at various time intervals (for example, with measurements every one, three or six days)

ACPD
15, 33209–33251, 2015

at different sites, and there were plenty of missing values at many sites. The observed concentrations are pre-processed following the two steps: (1) For a specific site, the observations are used in our analyses if the site had at least 5 months of observations and there were at least 5 days of observations within each month. (2) The mean seasonal cycle in aerosol concentrations in the months of November–March is removed by using the similar approach to that used for PNA index (see Sect. 2.3 below). Such deseasonality approach was used in previous studies that examined the monthly variations in mineral dust aerosol (Cakmur et al., 2001; Mahowald et al., 2003), the decreasing trends in observed $PM_{2.5}$ concentrations and satellite AOD in the southeastern US over 2000–2009 (Alston et al., 2012), and the monthly variations in global AOD (Li et al., 2013). The EPA-AQS sites with measurements that meet the criteria described in (1) are shown in Fig. 1.

2.2 GEOS-Chem simulation

We also examine the impacts of PNA on simulated aerosol concentrations in the US by using the GEOS-Chem model (version 8-2-1, http://acmg.seas.harvard.edu/geos). The GEOS-Chem model is a global chemical transport model driven by the assimilated meteorological fields from the Goddard Earth Observing System (GEOS) of the NASA Global Modeling and Assimilation Office (GMAO). The version of the model we use has a horizontal resolution of $2^{\circ} \times 2.5^{\circ}$ and 30 hybrid sigma-P layers from the surface to 0.01 hPa altitude. The model has a fully coupled simulation of tropospheric O_3-NO_x-VOC chemistry and aerosols including SO_4^{2-}, NO_3^-, NH_4^+, BC, OC (Park et al., 2003, 2004), mineral dust (Fairlie et al., 2007), and sea salt (Alexander et al., 2005). The model uses the advection scheme of Lin and Rood (1996), the deep convective scheme of Zhang and McFarlane (1995), the shallow convection scheme of Hack (1994), the wet deposition scheme of Liu et al. (2001), and the dry deposition scheme of Wesely (1989) and Wang et al. (1998). We mainly examine simulated anthropogenic aerosols from the GEOS-Chem simulation, since mineral dust concentrations in winter are very

ACPD
15, 33209–33251, 2015

small (Malm et al., 2004; Zhang et al., 2013) and sea salt is not a major aerosol species in the US (Malm et al., 2004).

We simulate aerosols for years of 1986–2006 driven by the GEOS-4 reanalysis data. The years of 1986–2006 are chosen for chemistry-aerosol simulation because these are the years that the GEOS-4 datasets are available. Global anthropogenic emissions are from the Global Emissions Inventory Activity (GEIA) (Park et al., 2004, 2006; Zhu et al., 2012; Yang et al., 2015). Anthropogenic emissions over the US are overwritten by the U.S. EPA National Emission Inventory for 1999 (NEI99), which have monthly variations in emissions of precursors including SO_2, NO_x, and NH_3. Monthly biomass burning emissions are taken from the Global Fire Emissions Database version 2 (GFED-2) (Giglio et al., 2006; van der Werf et al., 2006). During the simulation of aerosols for years of 1986–2006, the global anthropogenic and biomass burning emissions of aerosols and aerosol precursors are fixed at year 2005 levels, so that the variations in aerosol concentrations are caused by variations in meteorological parameters (PNA phases) alone.

Natural emissions of O_3 precursors, including biogenic NMVOCs and NO_x from lighting and soil, are allowed to vary over 1986–2006 following the variations in the GEOS-4 meteorological parameters. Biogenic NMVOC emissions are calculated using the module of Model of Emissions of Gases and Aerosols from Nature (Guenther et al., 2006). Lightning NO_x emissions are described by Sauvage et al. (2007) and Murray et al. (2012). Soil NO_x emissions are calculated using the algorithm proposed by Yienger and Levy (1995).

The GEOS-Chem simulation of aerosols in the US have been evaluated extensively by previous studies (Park et al., 2003, 2004, 2005; Heald et al., 2006; van Donkelaar et al., 2006; Liao et al., 2007; Heald et al., 2008; van Donkelaar et al., 2008; Fu et al., 2009; Drury et al., 2010; Leibensperger et al., 2011; Zhang et al., 2012). These studies have shown that the GEOS-Chem model can capture the magnitudes and distributions of aerosols in the US.

ACPD
15, 33209–33251, 2015

2.3 PNA index

The PNA index (PNAI) is commonly used to quantify the changes in PNA phase (Wallace and Gutzler, 1981; Leathers et al., 1991). This study follows the definition of PNAI by Leathers et al. (1991). In order to examine the monthly variations in PNA, the mean seasonal cycle of geopotential height at 700 hPa is removed for the months of November, December, January, February, and March (NDJFM) in the studied years. Such deseasonality approach has been used in the analyses of the growth and decay of PNA phase in NDJFM (Feldstein, 2002), the development of NAO (Feldstein, 2003), the influence of NAO on precipitation in Europe (Qian et al., 2000), and the variations in Madden–Julian oscillation (Wheeler and Hendon, 2004). If we are concerned with the PANI during n years, the monthly PNAI in month j (j is one of the 5 months of NDJFM) of year i is calculated by:

$$\mathrm{PNAI} = \frac{1}{3}\left[-Z^{*\prime}_{i,j}(47.9^{\circ}N, 170^{\circ}W) + Z^{*\prime}_{i,j}(47.9^{\circ}N, 110^{\circ}W) - Z^{*\prime}_{i,j}(29.7^{\circ}\mathrm{N}, 86.3^{\circ}\mathrm{W})\right] \quad (1)$$

where $Z^{*\prime}_{i,j} = \frac{Z'_{i,j} - \frac{1}{n\times 5}\sum_{i=1}^{n}\sum_{j=1}^{5} Z'_{i,j}}{\frac{1}{n\times 5}\sum_{i=1}^{n}\sum_{j=1}^{5}\left(Z'_{i,j} - \frac{1}{n\times 5}\sum_{i=1}^{n}\sum_{j=1}^{5} Z'_{i,j}\right)}$ and $Z'_{i,j} = Z_{i,j} - \frac{1}{n}\sum_{i=1}^{n} Z_{i,j}$. Therefore, $Z'_{i,j}$ denotes the removal of seasonal cycle, and $Z^{*\prime}_{i,j}$ denotes the standardized anomaly of geopotential height at 700 hPa in month j of year i with seasonal-cycle removed.

The PNAI is calculated by using both the National Center of Environmental Prediction-Department of Energy Atmospheric Model Inter-comparison Project Reanalysis data (NCEP-2, horizontal resolution 2.5° × 2.5° globally, http://www.esrl.noaa.gov/psd/data/gridded/data.ncep.reanalysis2.html) for years of 1986–2013 (referred to as NCEP2-PNAI) and the GEOS-4 assimilated meteorological data (referred to as GEOS4-PNAI) for 1986–2006 (Fig. 2). Both series of PNA index show strong monthly variations (Fig. 2), and the GEOS4-PNAI agrees with NCEP2-PNAI over 1986–2006 with a high correlation coefficient of 0.99, indicating that the NCEP-2 and GEOS-4 datasets are consistent in representing the monthly variations of PNAI.

ACPD
15, 33209–33251, 2015

There are $n \times 5$ PANI values for n years, since we calculate PNAI for the months of NDJFM of each year. These $n \times 5$ PANI values are classified into 3 categories for our composite analyses of aerosol concentrations and meteorological parameters: the positive PNA months (PNA+) that are 25 % of the $n \times 5$ PANI months with the highest positive PANI values, the negative PNA months (PNA–) that are 25 % of the $n \times 5$ PANI months with the highest negative PANI values, and the rest months that are referred to as the transitional months (Fig. 2).

3 Impacts of PNA on observed aerosol concentrations and wintertime pollution days

3.1 Impacts of the PNA phase on observed aerosol concentrations

The measurements of $PM_{2.5}$ are available over 1999–2013, in which there were 18 PNA+ months and 18 PNA– months as shown in Fig. 2a. Figure 3 shows the differences in observed surface-layer $PM_{2.5}$ concentrations between the PNA+ and PNA– months (concentrations averaged over the 18 PNA+ months minus those averaged over the 18 PNA– months). Among 492 sites with $PM_{2.5}$ concentrations (Fig. 1), 47 % of which had statistically significant differences in $PM_{2.5}$ between PNA+ and PNA– months. Relative to the PNA– months, $PM_{2.5}$ concentrations in PNA+ months were higher in California, the contiguous Salt Lake, and over and near the eastern Midwest. The enhancement of $PM_{2.5}$ reached 8–10 $\mu g\,m^{-3}$ (or 60–80 %) in California, 8–10 $\mu g\,m^{-3}$ (80–100 %) around the Salt Lake, 4–6 $\mu g\,m^{-3}$ (40–60 %) over and near the eastern Midwest. At sites in North Dakota, South Dakota, Minnesota, Montana, Texas and Maine, the $PM_{2.5}$ concentrations were lower by up to 4 $\mu g\,m^{-3}$ (–10 to –30 %) in PNA+ months than in PNA– months. As the concentrations are averaged over all sites (including the sites that pass and do not pass the t test with 90 % confidence level) in the US, the western US (west of 100° W, Fig. 1), and the eastern US (east of 100° W, Fig. 1), $PM_{2.5}$ concentrations were higher by 1.4 $\mu g\,m^{-3}$ (12.7 %), 2.0 $\mu g\,m^{-3}$ (21.9 %),

ACPD
15, 33209–33251, 2015

and 1.3 $\mu g\,m^{-3}$ (10.7 %), respectively, in the PNA+ months than in PNA– months (Table 1).

The measurements of speciated aerosols are available during 2000–2013, in which there were 17 PNA+ and 17 PNA– months (Fig. 2b). Figure 3 also shows the differences in observed surface-layer concentrations of individual aerosol species between the PNA+ and PNA– months. The differences in concentrations of SO_4^{2-}, NO_3^-, and NH_4^+ show statistically significant positive values at most sites. Among the 343, 355, and 194 sites with measurements of SO_4^{2-}, NO_3^-, and NH_4^+, 32, 44 %, and 40 % of which pass the two-tail t test with 90 % confidence level, respectively. While the absolute differences in concentrations of SO_4^{2-}, NO_3^-, and NH_4^+ between PNA+ and PNA– were in the range of 0–1 $\mu g\,m^{-3}$ at most sites, the maximum differences reached 2–3 $\mu g\,m^{-3}$ (50–100 %) for SO_4^{2-} in Pennsylvania, 2–3 $\mu g\,m^{-3}$ (150–200 %) for NO_3^- in Indiana, Ohio, California, and the contiguous Salt Lake, and 1–2 $\mu g\,m^{-3}$ (50–100 %) for NH_4^+ in Indiana and Pennsylvania. Averaged over the sites with measurements, the absolute differences in concentrations of SO_4^{2-}, NO_3^-, and NH_4^+ between PNA+ and PNA– months were larger in the eastern US than in the western US. As shown in Table 1, the differences in the averaged concentrations of SO_4^{2-}, NO_3^-, and NH_4^+ were, respectively, 0.3 $\mu g\,m^{-3}$ (10.7 %), 0.5 $\mu g\,m^{-3}$ (47.3 %), and 0.3 $\mu g\,m^{-3}$ (21.0 %) in the eastern US, 0.1 $\mu g\,m^{-3}$ (7.3 %), 0.2 $\mu g\,m^{-3}$ (33.1 %), and 0.3 $\mu g\,m^{-3}$ (43.6 %) in the western US, as well as 0.1 $\mu g\,m^{-3}$ (6.4 %), 0.3 $\mu g\,m^{-3}$ (39.1 %), and 0.2 $\mu g\,m^{-3}$ (22.8 %) in the whole of US.

With regard to carbonaceous aerosols, among the 105 and 104 sites with measurements of OC and BC, 57 and 32 % of which pass the two-tail t test with 90 % confidence, respectively. The differences in concentrations of these two species between PNA+ and PNA– months show similar geographical pattern, with positive values at most sites but negative values in Michigan, New York, and the South Atlantic States. The maximum differences between the PNA+ and PNA– months reached 4–5 $\mu g\,m^{-3}$ in California (150–200 %) and Kentucky (100–150 %) for OC. Averaged over sites with

ACPD
15, 33209–33251, 2015

measurements available, the differences in OC and BC concentrations between the PNA+ and PNA– months were larger in the western US than in the eastern US (Table 1). Among all aerosol species listed in Table 1, OC exhibited the largest absolute differences between the PNA phases in the western US, because OC accounts for 25–65 % of $PM_{2.5}$ in the western US (Malm et al., 2004) and the OC observed by EPA-AQS network, which are located in urban and suburban settings, were higher than the observations by other long term networks in US (Malm et al., 2011; Rattigan et al., 2011; Hand et al., 2012b, 2014).

Observations from EPA-AQS datasets indicate the large impacts of PNA phase on aerosol concentrations in the US. It should be noted that, in our analyses above, the locations of measurements and the numbers of samples were different for different aerosol species. Therefore, model results from the GEOS-Chem simulation will be used to further analyze the impacts of PNA on aerosols in the US, as presented in the subsequent sections.

3.2 The impact of PNA on the number of exceedance days in winter

The PNA phase also influences the number of exceedance days (defined as days with daily mean $PM_{2.5}$ concentrations exceeding 35 $\mu g\,m^{-3}$, the National Ambient Air Quality Standard (NAAQS) set by EPA). Such impact of PNA phase at a specific site can be quantified by the difference in standardized monthly exceedance days (SME-days) between PNA+ and PNA– months. The SME-days is defined as:

$$\text{SME-days} = \frac{\text{Observed exceedance days during all the PNA + (or PNA−) months}}{\text{Days with observations during all the PNA + (or PNA−) months}} \times 30 \quad (2)$$

Here we assume that there are 30 days in a month and SME-days has a unit of days $month^{-1}$. Figure 4 shows the differences in SME-days in the US between the PNA+ and PNA– months. The pattern of the differences in SME-days was similar to that of the

ACPD
15, 33209–33251, 2015

differences in $PM_{2.5}$ concentrations (Fig. 3). The differences in SME-days reached 2–3 days over Iowa, and 5–6 days in California and around the Salt Lake, corresponding to the PNA-induced changes in OC and NO_3^- aerosols in these places (Fig. 3).

4 Impacts of PNA on simulated aerosol concentrations

4.1 Simulated aerosol concentrations and model evaluation

Figure 5a shows the simulated surface-layer concentrations of $PM_{2.5}$ (the sum of SO_4^{2-}, NO_3^-, NH_4^+, BC, and OC) and each aerosol species averaged over NDJFM of 1999–2006. These years are selected because they are the common years of model results and EPA-AQS observation datasets. The simulated $PM_{2.5}$ concentrations were higher in the eastern US than in the western US. The maximum surface $PM_{2.5}$ concentrations reached 14–16 $\mu g\,m^{-3}$ in Ohio and Pennsylvania. $PM_{2.5}$ concentrations in the western US were generally less than 4 $\mu g\,m^{-3}$, except for California where $PM_{2.5}$ concentrations were 2–6 $\mu g\,m^{-3}$. The distribution of SO_4^{2-} was similar to that of $PM_{2.5}$, with higher concentrations in the eastern US (1–8 $\mu g\,m^{-3}$) than in the western US (0–3 $\mu g\,m^{-3}$) due to the coal-fired power plants in the Midwest (Park et al., 2006). The concentrations of NO_3^- and NH_4^+ were the highest over and near the eastern Midwest, with values of 3–4 and 2–3 $\mu g\,m^{-3}$, respectively. The maximum OC concentrations were simulated to be 2–3 $\mu g\,m^{-3}$ in two regions, from Ohio to Massachusetts and from Alabama to South Carolina. The simulated BC concentrations in the US were 0–1 $\mu g\,m^{-3}$, except for the contiguous New York where BC concentrations reached 1–2 $\mu g\,m^{-3}$. The magnitudes and geographic distributions of SO_4^{2-}, NO_3^-, NH_4^+ concentrations simulated in our work are similar to those simulated by Park et al. (2006) and Pye et al. (2009), and our simulated OC and BC were similar to those reported by Park et al. (2003).

Figure 5b presents the scatter plots of the simulated concentrations vs. the EPA-AQS observations. The simulated $PM_{2.5}$ concentrations had normalized mean bias

ACPD
15, 33209–33251, 2015

(NMB = $\sum_{i=1}^{N}(S_i - O_i)/\sum_{i=1}^{N}(O_i) \times 100\,\%$, where S_i and O_i are the simulated and observed aerosol concentrations, respectively) of –34 % over the US, and the correlation coefficient between simulated and observed $PM_{2.5}$ concentrations was 0.54. The simulated wintertime SO_4^{2-}, NO_3^-, and NH_4^+ had NMBs of 23, –12 and 7 %, respectively. Similar bias in simulated SO_4^{2-} in December–January–February (DJF) was reported Park et al. (2006), as the GEOS-Chem model results were compared with observations from the Clean Air Status and Trends Network (CASTNET). The NMB in our simulated NO_3^- agrees closely with that in Pye et al. (2009), who presented a NMB of –6 % in simulated NO_3^- in DJF when the GEOS-Chem simulations were compared with the CASTNET observations for 1999–2001. Our model underestimates $PM_{2.5}$, SO_4^{2-}, NO_3^-, NH_4^+, OC and BC in the western US (Fig. 5b), which can be explained in part by the relatively high aerosol concentrations observed for this region from the EPA-AQS. Hand et al. (2014) compared the observed concentrations of aerosols from the EPA-AQS with those from the Interagency Monitoring of Protected Visual Environments (IMPROVE) for 2008–2011, and showed that the ratios of wintertime aerosol concentrations of ammonium sulfate, ammonium nitrate, OC, and BC from the EPA-AQS to those from the IMPROVE were, respectively, 2.3, 7.7, 8.3, and 13.1, as the concentrations were averaged over the western US.

Since this study is dedicated to examine the influence of PNA phase on the month-to-month variations of aerosol concentrations during wintertime, Fig. 5c compares, for each aerosol species, the deviation from the mean (DM) of observed concentration with that of simulated concentration for each winter month. The DM is defined as $\mathrm{DM}_i = \left(C_i - \frac{1}{n}\sum_{i=1}^{n} C_i\right) / \frac{1}{n}\sum_{i=1}^{n} C_i$, where C_i is the simulated average aerosol concentration over the US in month i, and n is the number of winter months examined (we consider the months of NDJFM over 1999–2006 for $PM_{2.5}$, and the months of NDJFM over 2000–2006 for SO_4^{2-}, NO_3^-, NH_4^+, BC, and OC). The model captures fairly well the peaks and troughs of DMs for $PM_{2.5}$, SO_4^{2-}, NO_3^-, and NH_4^+, with correlation

ACPD
15, 33209–33251, 2015

coefficients of 0.48, 0.57, 0.31, and 0.74, respectively. The model does not capture well the monthly variations of DMs of concentrations of OC and BC, because both anthropogenic and biomass burning emissions are fixed at year 2005 levels during our simulation over 1986–2006 to isolate the impacts of variations in meteorological parameters (PNA phases) on aerosols (see Sect. 2.2). Figure 5c also shows the monthly variations in DMs of biomass burning emissions of OC and BC by using biomass burning emissions in NDJFM over 2000–2006 from GFED v2. The correlation coefficients between biomass burning emissions and observed concentrations of OC and BC were 0.36 and 0.32, respectively, indicating that the observed variations in OC and BC were influenced by monthly and interannual variations in biomass burning.

4.2 Impact of PNA on simulated surface-layer aerosol concentrations

We have performed the GEOS-Chem simulation for years 1986–2006, in which there were 35 PNA+ and 35 PNA– months (Fig. 2). Figure 6a shows the concentrations of $PM_{2.5}$ and each aerosols species (SO_4^{2-}, NO_3^-, NH_4^+, BC, and OC) averaged over the PNA– months of 1986–2006. The magnitudes and geographic distributions of aerosol concentrations in PNA– months were similar to those averaged over NDJFM of years 1999–2006 in Fig. 5.

The simulated absolute and relative differences in aerosol concentrations between PNA+ and PNA– months are shown in Fig. 6b and c. The $PM_{2.5}$ concentrations over the US are simulated to increase in PNA+ relative to PNA– months. The maximum enhancement in $PM_{2.5}$ concentrations in PNA+ months was 1.8–2.4 $\mu g\,m^{-3}$ (20–40 %), located in the juncture of Tennessee and Arkansas. Note that the pattern of simulated differences in $PM_{2.5}$ between PNA+ and PNA– months was similar to that of observations (Fig. 3), except that the simulated differences were not large in California, mainly due to the underestimation of OC in California as compared to EPA-AQS data (Fig. 5b). The simulated $PM_{2.5}$ concentrations were higher by 0.6 $\mu g\,m^{-3}$ (12.2 %), 0.3 $\mu g\,m^{-3}$ (14.0 %), and 0.9 $\mu g\ m^{-3}$ (10.8 %) over the whole of, western, and eastern US, respectively, in the PNA+ months than in PNA– months (Table 2). The simulated

ACPD
15, 33209–33251, 2015

relative differences were close to those from observations (Table 1) in the eastern and whole of US, but the difference was smaller than that from observations in the western US.

Figure 6 also shows the differences in simulated surface-layer concentrations of SO_4^{2-}, NO_3^-, and NH_4^+ between the PNA+ and the PNA– months. The differences in concentrations of SO_4^{2-} were larger in the western than in the eastern US, with maximum enhancements of 0.4–0.8 $\mu g\,m^{-3}$ (20–40 %) over the West North Central States (South Dakota, Nebraska, Minnesota, Iowa, and Missouri). The differences in concentrations of NO_3^- and NH_4^+ between PNA+ and PNA– months had similar geographical patterns, with increases in concentrations in a large fraction of the eastern US and over a belt region along the Rocky Mountain in the western US. The increases in concentrations of NO_3^- and NH_4^+ over the eastern US in PNA+ months relative to PNA– months agreed very well with those seen in observations (Fig. 3). The differences in concentrations of SO_4^{2-}, NO_3^-, and NH_4^+ in the eastern US between the PNA+ and PNA– months were 0.2 $\mu g\,m^{-3}$ (4.0 %), 0.4 $\mu g\,m^{-3}$ (33.5 %), and 0.2 $\mu g\,m^{-3}$ (13.2 %), respectively (Table 2).

The differences in concentrations of OC and BC between PNA+ and PNA– months had similar geographical patterns, with large increases in concentrations over and near the eastern Midwest and the region from northwestern US to Texas. The maximum differences reached 0.2–0.4 $\mu g\,m^{-3}$ (10–20 %) and 0.1–0.2 $\mu g\,m^{-3}$ (20–40 %) in Illinois, Indiana and Ohio for OC and BC, respectively. The magnitudes of the differences in OC and BC were statistically significant but were smaller than the observations (Tables 1 and 2). The absolute differences in OC were less than 0.1 $\mu g\,m^{-3}$ in the western, eastern and whole of US due to the underestimation of OC in the simulation.

In summary, model results agreed with observations in that the concentrations of all aerosol species of SO_4^{2-}, NO_3^-, NH_4^+, BC, and OC averaged over the US were higher in PNA+ months than in PNA– months. Relative to the PNA– months, the average concentration of $PM_{2.5}$ over the US was higher by about 12–13 % based on both observed and simulated concentrations. Furthermore, simulated geographical patterns

ACPD
15, 33209–33251, 2015

of the differences in $PM_{2.5}$ and each aerosol species between the PNA+ and PNA– months were similar to those seen in observations, with the largest increases in aerosol concentrations in PNA+ months over and near the eastern Midwest.

5 Mechanisms for the impact of PNA on aerosol concentrations

5.1 The impact of PNA on transboundary transport of aerosols

The transboundary transport of pollutants to and from the US depends largely on winds in the free troposphere (Liang et al., 2004). Figure 7 shows the horizontal winds at 700 hPa averaged over the winter months of NDJFM of 1986–2006 and the corresponding differences between PNA+ and PNA– months on the basis of the GEOS-4 meteorological fields. Strong westerlies prevailed over the US in wintertime (Fig. 7a). Relative to the PNA– months, anomalous northeasterlies occurred over a large fraction of US in the PNA+ months. Anomalous anti-cyclonic circulation occurred near the northwestern US and anomalous cyclonic circulation occurred near the southeastern US (Fig. 7b), corresponding to the large positive and negative differences in geopotential height in these two regions (see auxiliary Fig. S1), respectively.

We also calculate mass fluxes of $PM_{2.5}$ at the four lateral boundaries (from the surface to 100 hPa) of the US for different PNA phases (Table 3). The domain of the box to represent the US is (75–120° W, 28–49° N), as shown in Fig. 7b. For $PM_{2.5}$ in wintertime, the inflow from the west boundary and the outflow from the east boundary had the largest absolute values (Table 3). Relative to the PNA– months, the inflow from the west boundary and the outflow from the east boundary in PNA+ months exhibited reductions of 17.1 and 12.8 $kg\,s^{-1}$, respectively (Table 3). The inflow flux from south boundary decreased by 19.3 $kg\,s^{-1}$, and the inflow flux from north boundary increased by 37.6 $kg\,s^{-1}$, leading to a net increase of inflow flux of 14.0 $kg\,s^{-1}$ in PNA+ months. Therefore, the transboundary transport has an overall effect of increasing $PM_{2.5}$ aerosols in the US in PNA+ months relative to PNA– months. The relative

ACPD
15, 33209–33251, 2015

change in net flux was 11.4 % ((PNA+ minus PNA−)×100 %/PNA−) (Table 3), coinciding well with the enhancement of 12–13 % in surface-layer $PM_{2.5}$ concentration averaged over the US (Tables 1 and 2).

5.2 Local changes in aerosol concentrations caused by the PNA

The PNA pattern is also associated with variations in meteorological variables such as temperature (Leathers et al., 1991; Konrad II 1998; Notaro et al., 2006; Knight et al., 2008; Liu et al., 2015; Ning and Bradley, 2014, 2015), precipitation (Leathers et al., 1991; Henderson and Robinson, 1994; Coleman and Rogers, 2003; Notaro et al., 2006; Archambault et al., 2008; Myoung and Deng, 2009; Ning and Bradley, 2014, 2015; Wise et al., 2015) and humidity (Sheridan, 2003; Coleman and Rogers, 2003; Knight et al., 2008) in US, which are expected to influence aerosol concentrations within the US through chemical reactions, transport, and deposition.

Figure 8 shows the composite differences, between the PNA+ and PNA− months, in surface air temperature (T), precipitation rate (PR), relative humidity (RH), surface wind speed (WS), and planetary boundary layer height (PBLH), based on the reanalyzed GEOS-4 datasets. Relative to PNA− months, temperatures were higher by 1–3 K over the northwestern US and lower by 1–4 K in the southeastern region. Such geographic distributions of temperature anomalies were attributed to the maritime warm air in the northwestern US accompanied by the enhanced tropospheric geopotential height in North America (Leathers et al., 1991; Sheridan, 2003; Liu et al., 2015; Ning and Bradley, 2015) (see also auxiliary Fig. 1d) and the more frequent outbreak of cold air in southeastern US accompanied by the depressed geopotential height (Konrad II 1998; Liu et al., 2015) (see also auxiliary Fig. 1d). The differences in precipitation between PNA+ and PNA− months reached –1.6 to –2.4 mm day^{-1} (–32 to –48 %) over and near the eastern Midwest, –2.4 to –3.2 mm day^{-1} (–48 to –64 %) in the northwestern US, and 1.6–2.4 mm day^{-1} (16–32 %) in the southeastern US. These effects of PNA on precipitation were similar to those obtained from wintertime station data by Leathers et al. (1991), Coleman and Rogers (2003) and Wise et al. (2015). With re-

ACPD
15, 33209–33251, 2015

spect to RH, the values in the eastern US were generally lower in the PNA+ months than in PNA– months, as a result of the reduced moisture flux from the Gulf of Mexico to the eastern US (Coleman and Rogers, 2003), where RH showed maximum reduction of –3 to –9 %. The enhancement of RH of up to 6–9 % in Texas, Oklahoma and New Mexico was due to the anomalous easterlies over the south central US (see Fig. 8), which diminished the influence of the dry air from the deserts of the southwestern US and northwestern Mexico in PNA+ months (Sheridan, 2003). The surface WS showed reductions in PNA+ months relative to PNA– months in two regions, one was the belt region along the Rocky Mountain from the northwestern US to Texas (with the maximum reductions of 1.5–2.0 $m\,s^{-1}$ (48–64 %)) and the other region, with a northeast-southwest orientation, was from Ohio to Louisiana (with maximum reductions of 0.5–1.0 $m\,s^{-1}$ (16–32 %)). The differences in PBLH between PNA+ and PNA– months were statistically significant in the western US and in the belt region from the northeastern US to the eastern Midwest, with the maximum reductions in PBLH of 75–100 m (15–20 %) and 75–100 m (10–15 %), respectively.

The comparisons of Fig. 6b with Fig. 8a indicate that the increases in $PM_{2.5}$ concentrations over and near the eastern Midwest in PNA+ months relative to the PNA– months can be attributed to the decreases in PR, WS and PBLH in these locations, since the changes in these three variables depressed wet deposition, local horizontal diffusion, and vertical diffusion of the surface aerosols, respectively. The increases in SO_4^{2-} in the western US (Fig. 6b) corresponded to the decreases in PR and PBLH and the increased temperature. The increases in temperature enhance chemical reaction rates (Aw and Kleeman, 2003; Dawson et al., 2007; Kleeman, 2008). In the eastern US, although PR, WS, and PBLH decreased over and near the eastern Midwest, the cooling in the eastern US might have offset the effects by PR, WS, and PBLH, inducing practically no changes in SO_4^{2-} in the eastern US. The large increases in NO_3^- and NH_4^+ in the southeastern US (Fig. 6b) can be attributed to the reduced surface temperature, which was favorable to the wintertime formation of NO_3^- and NH_4^+ (Dawson

ACPD
15, 33209–33251, 2015

et al., 2007). The differences in concentrations of OC and BC between PNA+ and PNA– corresponded well with the reduced PR, WS and PBLH.

In order to quantify the impacts of anomalies in meteorological parameters driven by PNA on concentrations of different aerosol species, the pattern correlation coefficients (PCC, http://glossary.ametsoc.org/wiki/Pattern_correlation) are calculated and shown in Table 4. These pattern correlation coefficients denote the relationship between the geographical distribution of anomalies of each of T, PR, RH, WS, and PBLH (Fig. 8b) and that of the differences in concentration of each aerosol species between PNA+ and PNA– months (Fig. 6c). As shown in Table 4, over the whole US, the PNA influenced SO_4^{2-} concentrations mainly through changes PBLH, PR, and T, with the highest PCC values of −0.43, −0.38, and +0.26, respectively. For NO_3^-, the PNA-induced variations in temperature had a strong negative correlation (PCC= −0.59) with the PNA-induced differences in concentrations, indicating that surface temperature was the dominant meteorological factor to influence NO_3^- concentrations. For NH_4^+, OC, and BC, PR and PBLH were the two variables that had the largest negative PCC values (Table 4). Note that PBLH was the most important meteorological variable for SO_4^{2-}, NH_4^+, OC and BC, which contributed to the high correlation between PBLH and $PM_{2.5}$.

6 Conclusions

This study examined the impacts of monthly variation in the PNA phase on wintertime surface-layer aerosol concentrations in the US by the analyses of EPA-AQS observations over 1999–2013 and model results for 1986–2006 from the global chemical transport model GEOS-Chem.

The composite analyses on the EPA-AQS observations showed that the average concentrations of $PM_{2.5}$, SO_4^{2-}, NO_3^-, NH_4^+, OC, and BC aerosols over the US were higher in the PNA+ months than in the PNA– months by 1.4 $\mu g\,m^{-3}$ (12.7 %), 0.1 $\mu g\,m^{-3}$ (6.4 %), 0.3 $\mu g\,m^{-3}$ (39.1 %), 0.2 $\mu g\,m^{-3}$ (22.8 %), 0.8 $\mu g\,m^{-3}$ (21.3 %), and 0.2 $\mu g\,m^{-3}$ (34.1 %), respectively. Regionally, the observed $PM_{2.5}$ concentrations were

ACPD
15, 33209–33251, 2015

higher by 4–6 $\mu g\,m^{-3}$ (40–60 %) over the Midwest, and by 8–10 $\mu g\,m^{-3}$ (80–100 %) around the Salt Lake, as the concentrations in PNA+ months were compared to those in PNA– months.

The impacts of PNA phase on aerosol concentrations were reproduced fairly well by the GEOS-Chem simulation with fixed anthropogenic emissions (the variations of aerosols concentrations were driven by changes in meteorological fields alone). Concentrations of SO_4^{2-}, NO_3^-, NH_4^+, BC, and OC averaged over the US were simulated to be higher in the PNA+ months than in PNA– months. The average concentration of $PM_{2.5}$ over the US was simulated to be 12.2 % higher in the PNA+ months relative to the PNA– months, in close agreement with the observations. Simulated geographical patterns of the differences in $PM_{2.5}$ and each aerosol species between the PNA+ and PNA– months were similar to those seen in observations. The largest increases in aerosol concentrations in the PNA+ months were simulated to be over and near the eastern Midwest, but the model results showed small PNA-induced changes in aerosol concentrations in the western US.

The mechanisms for the impacts of PNA on aerosol concentrations were examined. The transboundary transport was found to have an overall effect of increasing $PM_{2.5}$ aerosols in the US in the PNA+ months relative to PNA– months. Compared to the PNA– months, anomalous northeasterlies occurred over a large fraction of US, which led to a net increase in inflow flux of $PM_{2.5}$ of 14.0 $kg\,s^{-1}$ in PNA+ months. Regionally within the US, the PNA influenced aerosol concentrations through changes in precipitation rate (PR), planetary boundary layer height (PBLH), surface wind speed (WS), surface air temperature (T) and relative humidity (RH), as represented by the pattern correlation coefficients (PCCs). The PNA influenced SO_4^{2-} concentration mainly through changes PBLH, PR, and T, with the highest PCC values of −0.43, −0.38, and +0.26, respectively. For NO_3^-, the PNA-induced variations in temperature had a strong negative correlation (PCC = −0.59) with the PNA-induced differences in concentrations. For NH_4^+, OC, and BC, PR and PBLH were the two variables that had the largest negative

ACPD
15, 33209–33251, 2015

PCC values. Because PBLH was the most important meteorological variable for SO_4^{2-}, NH_4^+, OC and BC, which led to a high correlation between PBLH and $PM_{2.5}$.

Conclusions from this study have important implications for air quality in the US. Leathers and Palechi (1992) showed that the PNAI were generally low in 1947–1957 but consistently high in 1958–1987. The PNAI during 1948–2010 exhibited an increasing trend for positive phases and a decreasing trend for negative phases (Liu et al., 2015; Ning et al., 2015; http://research.jisao.washington.edu/data_sets/pna/#djf), indicating that wintertime particulate matter pollution in most areas of US deteriorated due to variations in PNA phase alone. Climate models projected that positive PNA phases would increase in the future because of the global warming (Kachi and Nitta, 1997; Müller and Roeckner, 2008; Zhou, 2014). Therefore, the trend in PNA pattern underlies the necessity of strict emission reduction strategies for greenhouse gases, aerosols, and aerosol precursors.

The Supplement related to this article is available online at doi:10.5194/acpd-15-33209-2015-supplement.

Acknowledgements. This work was supported by the National Basic Research Program of China (973 program, Grant 2014CB441202) and the Strategic Priority Research Program of the Chinese Academy of Sciences (Grant No. XDA05100503).

References

Alexander, B., Park, R. J., Jacob, D. J., Li, Q. B., Yantosca, R. M., Savarino, J., Lee, C. C. W., and Thiemens, M. H.: Sulfate formation in sea-salt aerosols: constraints from oxygen isotopes, J. Geophys. Res., 110, D10307, doi:10.1029/2004JD005659, 2005.

Alston, E. J., Sokolik, I. N., and Kalashnikova, O. V.: Characterization of atmospheric aerosol in the US Southeast from ground- and space-based measurements over the past decade, Atmos. Meas. Tech., 5, 1667–1682, doi:10.5194/amt-5-1667-2012, 2012.

ACPD
15, 33209–33251, 2015

Archambault, H. M., Bosart, L. F., Keyser, D., and Aiyyer, A. R.: Influence of large-scale flow regimes on cool-season precipitation in the Northeastern United States, Mon. Weather Rev., 136, 2945–2963, doi:10.1175/2007MWR2308.1, 2008.
Athanasiadis, P. J. and Ambaum, M. H. P.: Linear contributions of different time scales to teleconnectivity, J. Climate, 22, 3720–3728, doi:10.1175/2009JCLI2707.1, 2009.
Aw, J. and Kleeman, M. J.: Evaluating the first-order effect of intraannual temperature variability on urban air pollution, J. Geophys. Res., 108, 4365, doi:10.1029/2002JD002688, 2003.
Bauer, S. E., Koch, D., Unger, N., Metzger, S. M., Shindell, D. T., and Streets, D. G.: Nitrate aerosols today and in 2030: a global simulation including aerosols and tropospheric ozone, Atmos. Chem. Phys., 7, 5043–5059, doi:10.5194/acp-7-5043-2007, 2007.
Blackmon, M. L., Lee, Y.-H., and Wallace, J. M.: Horizontal Structure of 500 mb Height Fluctuations with Long, Intermediate and Short Time Scales, J. Atmos. Sci., 41, 961–980, doi:10.1175/1520-0469(1984)041<0961:HSOMHF>2.0.CO;2, 1984.
Cakmur, R. V., Miller, R. L., and Tegen, I.: A comparison of seasonal and interannual variability of soil dust aerosols over the Atlantic Ocean as inferred by the TOMS AI and AVHRR AOT retrievals, J. Geophys. Res., 106, 18287, doi:10.1029/2000JD900525, 2001.
Chen, J., Vaughan, J., Avise, J., O'Neill, S., and Lamb, B.: Enhancement and evaluation of the AIRPACT ozone and $PM_{2.5}$ forecast system for the Pacific Northwest, J. Geophys. Res.-Atmos., 113, 1–20, doi:10.1029/2007JD009554, 2008.
Coleman, J. S. M. and Rogers, J. C.: Ohio river valley winter moisture conditions associated with the Pacific–North American teleconnection pattern, J. Climate, 16, 969–981, doi:10.1175/1520-0442(2003)016<0969:ORVWMC>2.0.CO;2, 2003.
Dawson, J. P., Adams, P. J., and Pandis, S. N.: Sensitivity of $PM_{2.5}$ to climate in the Eastern US: a modeling case study, Atmos. Chem. Phys., 7, 4295–4309, doi:10.5194/acp-7-4295-2007, 2007.
Day, M. C. and Pandis, S. N.: Predicted changes in summertime organic aerosol concentrations due to increased temperatures, Atmos. Environ., 45, 6546–6556, doi:10.1016/j.atmosenv.2011.08.028, 2011.
Di Pierro, M., Jaeglé, L., and Anderson, T. L.: Satellite observations of aerosol transport from East Asia to the Arctic: three case studies, Atmos. Chem. Phys., 11, 2225–2243, doi:10.5194/acp-11-2225-2011, 2011.
Drury, E., Jacob, D. J., Spurr, R. J. D., Wang, J., Shinozuka, Y., Anderson, B. E., Clarke, A. D., Dibb, J., McNaughton, C., and Weber, R.: Synthesis of satellite (MODIS), aircraft (ICARTT),

ACPD
15, 33209–33251, 2015

and surface (IMPROVE, EPA-AQS, AERONET) aerosol observations over eastern North America to improve MODIS aerosol retrievals and constrain surface aerosol concentrations and sources, J. Geophys. Res., 115, D14204, doi:10.1029/2009JD012629, 2010.

Dutkiewicz, V. A., Das, M., and Husain, L.: The relationship between regional SO_2 emissions and downwind aerosol sulfate concentrations in the northeastern US, Atmos. Environ., 34, 1821–1832, doi:10.1016/S1352-2310(99)00334-9, 2000.

Fairlie, D. T., Jacob, D. J., and Park, R. J.: The impact of transpacific transport of mineral dust in the United States, Atmos. Environ., 41, 1251–1266, doi:10.1016/j.atmosenv.2006.09.048, 2007.

Feldstein, S. B.: Fundamental mechanisms of the growth and decay of the PNA teleconnection pattern, Q. J. Roy. Meteor. Soc., 128, 775–796, doi:10.1256/0035900021643683, 2002.

Feldstein, S. B.: The dynamics of NAO teleconnection pattern growth and decay, Q. J. Roy. Meteor. Soc., 129, 901–924, doi:10.1256/qj.02.76, 2003.

Fu, T.-M., Jacob, D. J., and Heald, C. L.: Aqueous-phase reactive uptake of dicarbonyls as a source of organic aerosol over eastern North America, Atmos. Environ., 43, 1814–1822, doi:10.1016/j.atmosenv.2008.12.029, 2009.

Giglio, L., van der Werf, G. R., Randerson, J. T., Collatz, G. J., and Kasibhatla, P.: Global estimation of burned area using MODIS active fire observations, Atmos. Chem. Phys., 6, 957–974, doi:10.5194/acp-6-957-2006, 2006.

Gong, S. L., Zhang, X. Y., Zhao, T. L., Zhang, X. B., Barrie, L. A., McKendry, I. G., and Zhao, C. S.: A simulated climatology of Asian dust aerosol and its Trans-Pacific transport. Part II: Interannual Variability and Climate Connections, J. Climate, 19, 104–122, doi:10.1175/JCLI3606.1, 2006.

Guenther, A., Karl, T., Harley, P., Wiedinmyer, C., Palmer, P. I., and Geron, C.: Estimates of global terrestrial isoprene emissions using MEGAN (Model of Emissions of Gases and Aerosols from Nature), Atmos. Chem. Phys., 6, 3181–3210, doi:10.5194/acp-6-3181-2006, 2006.

Hack, J. J.: Parameterization of moist convection in the National Center for Atmosphric Research community climate model (CCM2), J. Geophys. Res., 99, 5551, doi:10.1029/93JD03478, 1994.

Hand, J. L., Schichtel, B. A., Malm, W. C., and Pitchford, M. L.: Particulate sulfate ion concentration and SO_2 emission trends in the United States from the early 1990s through 2010, Atmos. Chem. Phys., 12, 10353–10365, doi:10.5194/acp-12-10353-2012, 2012a.

ACPD
15, 33209–33251, 2015

Hand, J. L., Schichtel, B. A., Pitchford, M., Malm, W. C., and Frank, N. H.: Seasonal composition of remote and urban fine particulate matter in the United States, J. Geophys. Res., 117, D05209, doi:10.1029/2011JD017122, 2012b.

Hand, J. L., Schichtel, B. A., Malm, W. C., Pitchford, M., and Frank, N. H.: Spatial and seasonal patterns in urban influence on regional concentrations of speciated aerosols across the United States, J. Geophys. Res.-Atmos., 119, 12832–12849, doi:10.1002/2014JD022328, 2014.

Heald, C. L., Jacob, D. J., Park, R. J., Alexander, B., Fairlie, T. D., Yantosca, R. M., and Chu, D. A.: Transpacific transport of Asian anthropogenic aerosols and its impact on surface air quality in the United States, J. Geophys. Res.-Atmos., 111, 1–13, doi:10.1029/2005JD006847, 2006.

Heald, C. L., Henze, D. K., Horowitz, L. W., Feddema, J., Lamarque, J.-F., Guenther, A., Hess, P. G., Vitt, F., Seinfeld, J. H., Goldstein, A. H., and Fung, I.: Predicted change in global secondary organic aerosol concentrations in response to future climate, emissions, and land use change, J. Geophys. Res.-Atmos., 113, D05211, doi:10.1029/2007JD009092, 2008.

Henderson, K. G. and Robinson, P. J.: Relationships between the pacific/north american teleconnection patterns and precipitation events in the south-eastern USA, Int. J. Climatol., 14, 307–323, doi:10.1002/joc.3370140305, 1994.

IPCC: Climate Change 2013 The Physical Science Basis: Working Group I Contribution to the Fifth Assessment Report of the Intergovernmental Panel on Climate Change, 1st Edn., Cambridge University Press, New York, available at: http://www.climatechange2013.org/images/report/WG1AR5_ALL_FINAL.pdf (last access: 20 November 2015), 2013.

Jacob, D. J. and Winner, D. A.: Effect of climate change on air quality, Atmos. Environ., 43, 51–63, doi:10.1016/j.atmosenv.2008.09.051, 2009.

Jaffe, D., Tamura, S., and Harris, J.: Seasonal cycle and composition of background fine particles along the west coast of the US, Atmos. Environ., 39, 297–306, doi:10.1016/j.atmosenv.2004.09.016, 2005.

Jerez, S., Jimenez-Guerrero, P., Montávez, J. P., and Trigo, R. M.: Impact of the North Atlantic Oscillation on European aerosol ground levels through local processes: a seasonal model-based assessment using fixed anthropogenic emissions, Atmos. Chem. Phys., 13, 11195–11207, doi:10.5194/acp-13-11195-2013, 2013.

Juda-Rezler, K., Reizer, M., Huszar, P., Krüger, B., Zanis, P., Syrakov, D., Katragkou, E., Trapp, W., Melas, D., Chervenkov, H., Tegoulias, I., and Halenka, T.: Modelling the effects

ACPD
15, 33209–33251, 2015

of climate change on air quality over Central and Eastern Europe: concept, evaluation and projections, Clim. Res., 53, 179–203, doi:10.3354/cr01072, 2012.
Kachi, M. and Nitta, T.: Decadal variations of the global atmosphere–ocean system, J. Meteorol. Soc. Jpn., 75, 657–675, 1997.
Kleeman, M. J.: A preliminary assessment of the sensitivity of air quality in California to global change, Clim. Change, 87, 273–292, doi:10.1007/s10584-007-9351-3, 2008.
Knight, D. B., Davis, R. E., Sheridan, S. C., Hondula, D. M., Sitka, L. J., Deaton, M., Lee, T. R., Gawtry, S. D., Stenger, P. J., Mazzei, F., and Kenny, B. P.: Increasing frequencies of warm and humid air masses over the conterminous United States from 1948 to 2005, Geophys. Res. Lett., 35, L10702, doi:10.1029/2008GL033697, 2008.
Konrad II, C. E.: Persistent planetary scale circulation patterns and their relationship with cold air outbreak activity over the Eastern United States, Int. J. Climatol., 18, 1209–1221, doi:10.1002/(SICI)1097-0088(199809)18:11<1209::AID-JOC301>3.0.CO;2-K, 1998.
Lam, Y. F., Fu, J. S., Wu, S., and Mickley, L. J.: Impacts of future climate change and effects of biogenic emissions on surface ozone and particulate matter concentrations in the United States, Atmos. Chem. Phys., 11, 4789–4806, doi:10.5194/acp-11-4789-2011, 2011.
Leathers, D. J. and Palecki, M. A.: The Pacific/North American teleconnection pattern and United States climate. Part II: Temporal characteristics and index specification, J. Climate, 5, 707–716, doi:10.1175/1520-0442(1992)005<0707:TPATPA>2.0.CO;2, 1992.
Leathers, D. J., Yarnal, B., and Palecki, M. A.: The Pacific/North American teleconnection pattern and United States climate. Part I: Regional temperature and precipitation associations, J. Climate, 4, 517–528, doi:10.1175/1520-0442(1991)004<0517:TPATPA>2.0.CO;2, 1991.
Leibensperger, E. M., Mickley, L. J., Jacob, D. J., and Barrett, S. R. H.: Intercontinental influence of NO_x and CO emissions on particulate matter air quality, Atmos. Environ., 45, 3318–3324, doi:10.1016/j.atmosenv.2011.02.023, 2011.
Li, J., Carlson, B. E., and Lacis, A. A.: Application of spectral analysis techniques in the intercomparison of aerosol data: 1. An EOF approach to analyze the spatial–temporal variability of aerosol optical depth using multiple remote sensing data sets, J. Geophys. Res.-Atmos., 118, 8640–8648, doi:10.1002/jgrd.50686, 2013.
Liang, Q., Jaeglé, L., Jaffe, D. A., Weiss-Penzias, P., Heckman, A., and Snow, J. A.: Long-range transport of Asian pollution to the northeast Pacific: seasonal variations and transport pathways of carbon monoxide, J. Geophys. Res.-Atmos., 109, 1–16, doi:10.1029/2003JD004402, 2004.

ACPD
15, 33209–33251, 2015

Liang, Q., Jaeglé, L., and Wallace, J. M.: Meteorological indices for Asian outflow and transpacific transport on daily to interannual timescales, J. Geophys. Res., 110, D18308, doi:10.1029/2005JD005788, 2005.
Liao, H., Chen, W. T., and Seinfeld, J. H.: Role of climate change in global predictions of future tropospheric ozone and aerosols, J. Geophys. Res.-Atmos., 111, 1–18, doi:10.1029/2005JD006852, 2006.
Liao, H., Henze, D. K., Seinfeld, J. H., Wu, S., and Mickley, L. J.: Biogenic secondary organic aerosol over the United States: comparison of climatological simulations with observations, J. Geophys. Res., 112, D06201, doi:10.1029/2006JD007813, 2007.
Lin, S.-J., and Rood, R. B.: Multidimensional flux-form semi-lagrangian transport schemes, Mon. Weather Rev., 124, 2046–2070, doi:10.1175/1520-0493(1996)124<2046:MFFSLT>2.0.CO;2, 1996.
Liu, H.-Y., Jacob, D. J., Bey, I., and Yantosca, R. M.: Constraints Pb-210 and Be-7 on Wet deposition and transport in a global three-dimensional chemical tracer model driven by assimilated meteorological fields, J. Geophys. Res. Atmos., 106, 12109–12128, doi:10.1029/2000JD900839, 2001.
Liu, Y., Liu, J., and Tao, S.: Interannual variability of summertime aerosol optical depth over East Asia during 2000–2011: a potential influence from El Niño Southern Oscillation, Environ. Res. Lett., 8, 044034, doi:10.1088/1748-9326/8/4/044034, 2013.
Liu, Z., Jian, Z., Yoshimura, K., Buenning, N. H., Poulsen, C. J., and Bowen, G. J.: Recent contrasting winter temperature changes over North America linked to enhanced positive Pacific-North American pattern, Geophys. Res. Lett., 42, 1–8, doi:10.1002/2015GL065656, 2015.
Mahowald, N., Luo, C., del Corral, J., Zender, C. S.: Interannual variability in atmospheric mineral aerosols from a 22 year model simulation and observational data, J. Geophys. Res., 108, 4352, doi:10.1029/2002JD002821, 2003.
Malm, W. C.: Spatial and monthly trends in speciated fine particle concentration in the United States, J. Geophys. Res., 109, D03306, doi:10.1029/2003JD003739, 2004.
Malm, W. C., Schichtel, B. A., and Pitchford, M. L.: Uncertainties in $PM_{2.5}$ gravimetric and speciation measurements and what we can learn from them, JAPCA J. Air Waste Ma., 61, 1131–1149, doi:10.1080/10473289.2011.603998, 2011.
Mijling, B., van der A, R. J., and Zhang, Q.: Regional nitrogen oxides emission trends in East Asia observed from space, Atmos. Chem. Phys., 13, 12003–12012, doi:10.5194/acp-13-12003-2013, 2013.

ACPD
15, 33209–33251, 2015

Moulin, C. and Lambert, C. E., Dulac, F., and Dayan, U.: Control of atmospheric export of dust from North Africa by the North Atlantic Oscillation, Nature, 387, 691–694, 1997.
Müller, W. A. and Roeckner, E.: ENSO teleconnections in projections of future climate in ECHAM5/MPI-OM, Clim. Dynam., 31, 533–549, doi:10.1007/s00382-007-0357-3, 2008.
Murray, L. T., Jacob, D. J., Logan, J. A., Hudman, R. C., and Koshak, W. J.: Optimized regional and interannual variability of lightning in a global chemical transport model constrained by LIS/OTD satellite data, J. Geophys. Res.-Atmos., 117, D20307, doi:10.1029/2012JD017934, 2012.
Myoung, B. and Deng, Y.: Interannual Variability of the Cyclonic Activity along the US Pacific Coast: influences on the Characteristics of Winter Precipitation in the Western United States, J. Climate, 22, 5732–5747, doi:10.1175/2009JCLI2889.1, 2009.
Ning, L. and Bradley, R. S.: Winter precipitation variability and corresponding teleconnections over the northeastern United States, J. Geophys. Res. Atmos., 119, 7931–7945, doi:10.1002/2014JD021591, 2014.
Ning, L. and Bradley, R. S.: Winter Climate Extremes over the Northeastern United States and Southeastern Canada and Teleconnections with Large-Scale Modes of Climate Variability, J. Climate, 28, 2475–2493, doi:10.1175/JCLI-D-13-00750.1, 2015.
Notaro, M., Wang, W.-C., and Gong, W.: Model and observational analysis of the Northeast US regional climate and its relationship to the PNA and NAO patterns during early winter, Mon. Weather Rev., 134, 3479–3505, doi:10.1175/MWR3234.1, 2006.
Park, R. J., Jacob, D. J., Chin, M., and Martin, R. V.: Sources of carbonaceous aerosols over the United States and implications for natural visibility, J. Geophys. Res., 108, 4355, doi:10.1029/2002JD003190, 2003.
Park, R. J., Jacob, D. J., Field, B. D., Yantosca, R. M., and Chin, M.: Natural and transboundary pollution influences on sulfate-nitrate-ammonium aerosols in the United States: implications for policy, J. Geophys. Res., 109, D15204, doi:10.1029/2003JD004473, 2004.
Park, R. J., Jacob, D. J., Palmer, P. I., Clarke, A. D., Weber, R. J., Zondlo, M. A., Eisele, F. L., Bandy, A. R., Thornton, D. C., Sachse, G. W., and Bond, T. C.: Export efficiency of black carbon aerosol in continental outflow: global implications, J. Geophys. Res.-Atmos., 110, 1–7, doi:10.1029/2004JD005432, 2005.
Park, R. J., Jacob, D. J., Kumar, N., and Yantosca, R. M.: Regional visibility statistics in the United States: natural and transboundary pollution influences, and implications for the Re-

ACPD
15, 33209–33251, 2015

gional Haze Rule, Atmos. Environ., 40, 5405–5423, doi:10.1016/j.atmosenv.2006.04.059, 2006.

Pye, H. O. T., Liao, H., Wu, S., Mickley, L. J., Jacob, D. J., Henze, D. K., and Seinfeld, J. H.: Effect of changes in climate and emissions on future sulfate-nitrate-ammonium aerosol levels in the United States, J. Geophys. Res., 114, D01205, doi:10.1029/2008JD010701, 2009.

Qian, B., Corte-Real, J., and Xu, H.: Is the North Atlantic Oscillation the most important atmospheric pattern for precipitation in Europe?, J. Geophys. Res., 105, 11901, doi:10.1029/2000JD900102, 2000.

Rattigan, O. V., Felton, H. D., Bae, M.-S., Schwab, J. J., and Demerjian, K. L.: Comparison of long-term $PM_{2.5}$ carbon measurements at an urban and rural location in New York, Atmos. Environ., 45, 3228–3236, doi:10.1016/j.atmosenv.2011.03.048, 2011.

Redmond, K. T. and Koch, R. W.: Surface climate and streamflow variability in the Western United States and their relationship to large-scale circulation indices, Water Resour. Res., 27, 2381–2399, doi:10.1029/91WR00690, 1991.

Sauvage, B., Martin, R. V., van Donkelaar, A., Liu, X., Chance, K., Jaeglé, L., Palmer, P. I., Wu, S., and Fu, T.-M.: Remote sensed and in situ constraints on processes affecting tropical tropospheric ozone, Atmos. Chem. Phys., 7, 815–838, doi:10.5194/acp-7-815-2007, 2007.

Sheridan, S. C.: North American weather-type frequency and teleconnection indices, Int. J. Climatol., 23, 27–45, doi:10.1002/joc.863, 2003.

Singh, A. and Palazoglu, A.: Climatic variability and its influence on ozone and PM pollution in 6 non-attainment regions in the United States, Atmos. Environ., 51, 212–224, doi:10.1016/j.atmosenv.2012.01.020, 2012.

Tai, A. P. K., Mickley, L. J., and Jacob, D. J.: Correlations between fine particulate matter ($PM_{2.5}$) and meteorological variables in the United States: implications for the sensitivity of $PM_{2.5}$ to climate change, Atmos. Environ., 44, 3976–3984, doi:10.1016/j.atmosenv.2010.06.060, 2010.

Tai, A. P. K., Mickley, L. J., Jacob, D. J., Leibensperger, E. M., Zhang, L., Fisher, J. A., and Pye, H. O. T.: Meteorological modes of variability for fine particulate matter ($PM_{2.5}$) air quality in the United States: implications for $PM_{2.5}$ sensitivity to climate change, Atmos. Chem. Phys., 12, 3131–3145, doi:10.5194/acp-12-3131-2012, 2012a.

Tai, A. P. K., Mickley, L. J., and Jacob, D. J.: Impact of 2000–2050 climate change on fine particulate matter ($PM_{2.5}$) air quality inferred from a multi-model analysis of meteorological modes, Atmos. Chem. Phys., 12, 11329–11337, doi:10.5194/acp-12-11329-2012, 2012b.

ACPD
15, 33209–33251, 2015

Unger, N., Shindell, D. T., Koch, D. M., Amann, M., Cofala, J., and Streets, D. G.: Influences of man-made emissions and climate changes on tropospheric ozone, methane, and sulfate at 2030 from a broad range of possible futures, J. Geophys. Res., 111, D12313, doi:10.1029/2005JD006518, 2006.

van der Werf, G. R., Randerson, J. T., Giglio, L., Collatz, G. J., Kasibhatla, P. S., and Arellano Jr., A. F.: Interannual variability in global biomass burning emissions from 1997 to 2004, Atmos. Chem. Phys., 6, 3423–3441, doi:10.5194/acp-6-3423-2006, 2006.

van Donkelaar, A., Martin, R. V., and Park, R. J.: Estimating ground-level $PM_{2.5}$ using aerosol optical depth determined from satellite remote sensing, J. Geophys. Res., 111, D21201, doi:10.1029/2005JD006996, 2006.

van Donkelaar, A., Martin, R. V., Leaitch, W. R., Macdonald, A. M., Walker, T. W., Streets, D. G., Zhang, Q., Dunlea, E. J., Jimenez, J. L., Dibb, J. E., Huey, L. G., Weber, R., and Andreae, M. O.: Analysis of aircraft and satellite measurements from the Intercontinental Chemical Transport Experiment (INTEX-B) to quantify long-range transport of East Asian sulfur to Canada, Atmos. Chem. Phys., 8, 2999–3014, doi:10.5194/acp-8-2999-2008, 2008.

Vestreng, V., Myhre, G., Fagerli, H., Reis, S., and Tarrasón, L.: Twenty-five years of continuous sulphur dioxide emission reduction in Europe, Atmos. Chem. Phys., 7, 3663–3681, doi:10.5194/acp-7-3663-2007, 2007.

Wallace, J. M. and Gutzler, D. S.: Teleconnections in the geopotential height field during the Northern Hemisphere winter, Mon. Weather Rev., 109, 784–812, doi:10.1175/1520-0493(1981)109<0784:TITGHF>2.0.CO;2, 1981.

Wang, Y., Logan, J. A., and Jacob, D. J.: Global simulation of tropospheric O_3-NO_x-hydrocarbon chemistry: 2. Model evaluation and global ozone budget, J. Geophys. Res., 103, 10727, doi:10.1029/98JD00157, 1998.

Wesely, M. L.: Parameterization of surface resistances to gaseous dry deposition in regional-scale numerical models, Atmos. Environ., 23, 1293–1304, doi:10.1016/0004-6981(89)90153-4, 1989.

Wheeler, M. C. and Hendon, H. H.: An all-season real-time multivariate MJO index: development of an index for monitoring and prediction, Mon. Weather Rev., 132, 1917–1932, doi:10.1175/1520-0493(2004)132<1917:AARMMI>2.0.CO;2, 2004.

Wise, E. K. and Comrie, A. C.: Meteorologically adjusted urban air quality trends in the Southwestern United States, Atmos. Environ., 39, 2969–2980, doi:10.1016/j.atmosenv.2005.01.024, 2005.

ACPD
15, 33209–33251, 2015

Yang, Y., Liao, H., and Lou, S.: Decadal trend and interannual variation of outflow of aerosols from East Asia: roles of variations in meteorological parameters and emissions, Atmos. Environ., 100, 141–153, doi:10.1016/j.atmosenv.2014.11.004, 2015.

Yienger, J. J. and Levy, H.: Empirical model of global soil-biogenic NO_x emissions, J. Geophys. Res., 100, 11447, doi:10.1029/95JD00370, 1995.

Zhang, G. J. and McFarlane, N. A.: Sensitivity of climate simulations to the parameterization of cumulus convection in the Canadian climate centre general circulation model, Atmos. Ocean, 33, 407–446, doi:10.1080/07055900.1995.9649539, 1995.

Zhang, L., Jacob, D. J., Knipping, E. M., Kumar, N., Munger, J. W., Carouge, C. C., van Donkelaar, A., Wang, Y. X., and Chen, D.: Nitrogen deposition to the United States: distribution, sources, and processes, Atmos. Chem. Phys., 12, 4539–4554, doi:10.5194/acp-12-4539-2012, 2012.

Zhang, L., Kok, J. F., Henze, D. K., Li, Q., and Zhao, C.: Improving simulations of fine dust surface concentrations over the western United States by optimizing the particle size distribution, Geophys. Res. Lett., 40, 3270–3275, doi:10.1002/grl.50591, 2013.

Zhou, Z.-Q., Xie, S.-P., Zheng, X.-T., Liu, Q., and Wang, H.: Global warming–induced changes in El Niño teleconnections over the North Pacific and North America, J. Climate, 27, 9050–9064, doi:10.1175/JCLI-D-14-00254.1, 2014.

Zhu, J., Liao, H., and Li, J.: Increases in aerosol concentrations over eastern China due to the decadal-scale weakening of the East Asian summer monsoon, Geophys. Res. Lett., 39, L09809, doi:10.1029/2012GL051428, 2012.

ACPD
15, 33209–33251, 2015

Table 1. The absolute ($\mu g\,m^{-3}$) and relative (%) differences in observed aerosol concentrations between the PNA+ and PNA– months (PNA+ minus PNA–). The observed concentrations are averaged over all the sites in the whole of US, in the western US, or in the eastern US. See Fig. 1 for locations of the sites. The measurements are from the EPA-AQS data. The ** and * indicate the differences that have passed the two-tail Student *t* test with 95 and 90 % significance levels, respectively.

	Whole US	Western US	Eastern US
$PM_{2.5}$	1.4 (12.7 %)**	2.0 (21.9 %)**	1.3 (10.7 %)**
SO_4^{2-}	0.1 (6.4 %)	0.1 (7.3 %)	0.3 (10.7 %)*
NO_3^-	0.3 (39.1 %)**	0.2 (33.1 %)**	0.5 (47.3 %)**
NH_4^+	0.2 (22.8 %)**	0.3 (43.6 %)**	0.3 (21.0 %)**
OC	0.8 (21.3 %)**	1.5 (31.4 %)*	0.5 (12.8 %)**
BC	0.2 (34.1 %)**	0.2 (32.2 %)**	0.2 (30.0 %)**

ACPD
15, 33209–33251, 2015

Table 2. The absolute ($\mu g\,m^{-3}$) and relative (%) differences in simulated aerosol concentrations between the PNA+ and PNA– months (PNA+ minus PNA–). The simulated concentrations are averaged over the whole of US, the western US (west of 100° W), or the eastern US (east of 100° W). The concentrations are from the GEOS-Chem simulation for 1986–2006. The ** and * indicate the differences that have passed the two-tail Student *t* test with 95 and 90 % significance levels, respectively.

	Whole US	Western US	Eastern US
$PM_{2.5}$	0.6 (12.2 %)**	0.3 (14.0 %)**	0.9 (10.8 %)**
SO_4^{2-}	0.2 (7.1 %)	0.1 (13.5 %) **	0.2 (4.0 %)
NO_3^-	0.2 (30.3 %) **	0.1 (28.5 %) **	0.4 (33.5 %)**
NH_4^+	0.2 (14.4 %)**	0.1 (15.4 %)**	0.2 (13.2 %)**
OC	0.05 (6.5 %)**	0.03 (8.6 %)**	0.08 (5.9 %)**
BC	0.03 (10.2 %)**	0.01 (8.6 %)**	0.05 (11.0 %)**

ACPD
15, 33209–33251, 2015

Table 3. The composite analyses of horizontal mass fluxes ($kg\,s^{-1}$) of $PM_{2.5}$ for the selected box of (75–120° W, 28–49° N, from the surface to 100 hPa) in the PNA+ and PNA– months of 1986–2006. The positive values at the four boundaries indicate eastward or northward transport, and negative values indicate westward or southward transport. The positive (negative) value of net flux indicates the net gain (loss) of $PM_{2.5}$ in the selected box. All the fluxes are from the GEOS-Chem simulation.

	Boundaries and total	Mass Flux
PNA+	West	89.7
	East	259.3
	South	24.4
	North	–36.2
	Net flux	–109.0
PNA–	West	106.8
	East	272.1
	South	43.7
	North	1.4
	Net flux	–123.0
Diff. (PNA+ minus PNA–)	West	–17.1
	East	–12.8
	South	–19.3
	North	–37.6
	Net flux	14.0

ACPD
15, 33209–33251, 2015

Table 4. The pattern correlation coefficients between the composite differences in aerosol concentrations (Fig. 6c) and the corresponding composite differences in meteorological parameters (Fig. 8b). The * denotes the correlations that have passed the two-tail *t* test with 95 % confidence level.

	$PM_{2.5}$	SO_4^{2-}	NO_3^-	NH_4	OC	BC
T	–0.13	0.26*	–0.59*	–0.22*	0.07	–0.16
PR	–0.44*	–0.38*	0.04	–0.42*	–0.63*	–0.50*
RH	–0.08	–0.05	–0.02	0.12	–0.32*	–0.36*
WS	–0.27*	–0.1	–0.22*	–0.27*	–0.28*	–0.24*
PBLH	–0.61*	–0.43*	–0.32*	–0.61*	–0.60*	–0.55*

ACPD
15, 33209–33251, 2015

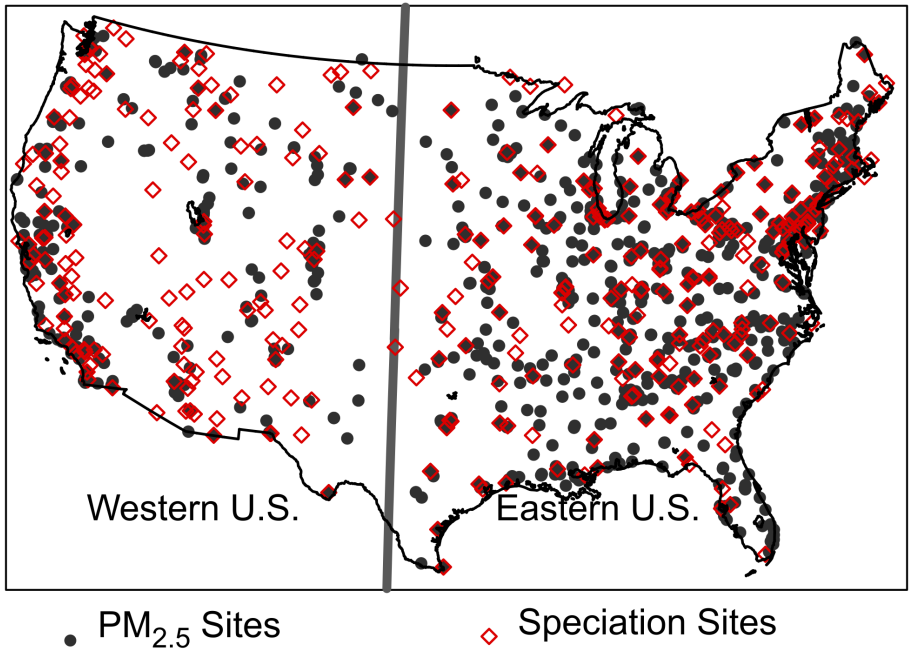

Figure 1. The locations of EPA-AQS sites with measurements that meet the criteria described in Sect. 2.1 in the text. $PM_{2.5}$ measurements are available for years of 1999–2013 (sites are marked by black dots) and speciated aerosol (SO_4^{2-}, NO_3^-, NH_4^+, BC, and OC) concentrations are available over years of 2000–2013 (sites are marked by red diamonds). The grey solid line defines the western United States (west of 100° W) and eastern United States (east of 100° W).

ACPD
15, 33209–33251, 2015

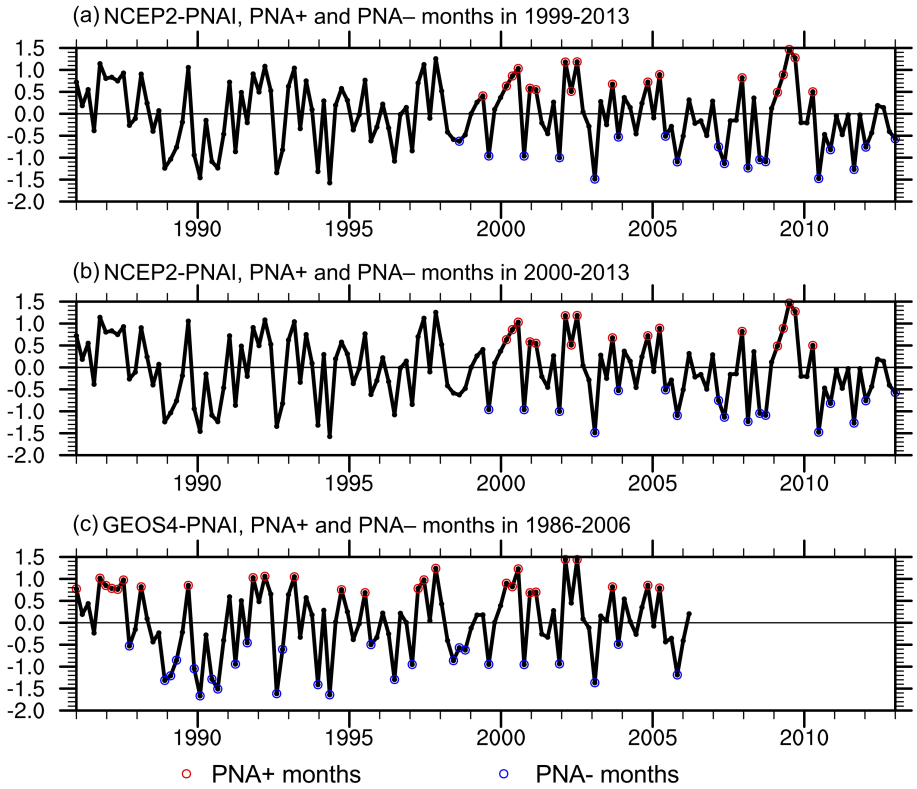

Figure 2. (a) PNAI for years of 1986–2013 calculated using the NCEP-2 data (NCEP2-PNAI), with the PNA+ and PNA– months during 1999–2013 indicated. **(b)** PNAI for years of 1986–2013 calculated using the NCEP-2 data, with the PNA+ and PNA– months during 2000–2013 indicated. **(c)** PNAI for years of 1986–2006 calculated using the GEOS-4 data (GEOS4-PNAI), with the PNA+ and PNA– months over 1986–2006 indicated. Red circles are PNA+ months and blue circles PNA– months.

ACPD
15, 33209–33251, 2015

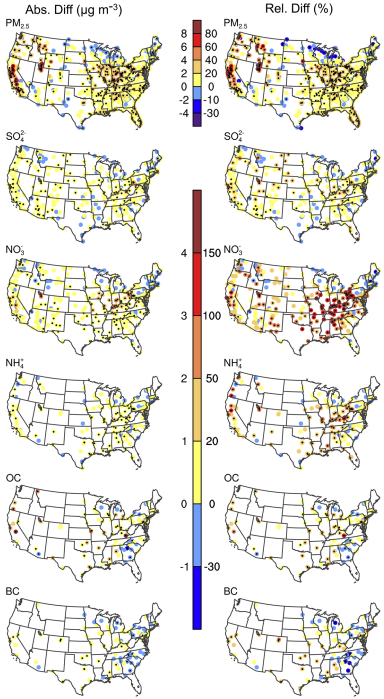

Figure 3. The absolute (μg m^{-3}, left column) and relative differences (%, right column) in observed aerosol concentrations between PNA+ and PNA− months (PNA+ minus PNA−). The measurements of $PM_{2.5}$ were carried out over 1999–2013, in which there were 18 PNA+ months and 18 PNA− months as shown in Fig. 2a. The measurements of speciated aerosols were taken during 2000–2013, in which there were 17 PNA+ and 17 PNA− months (Fig. 2b). The sites with black dots are those that have passed the two-tail t test with 90 % confidence level.

ACPD
15, 33209–33251, 2015

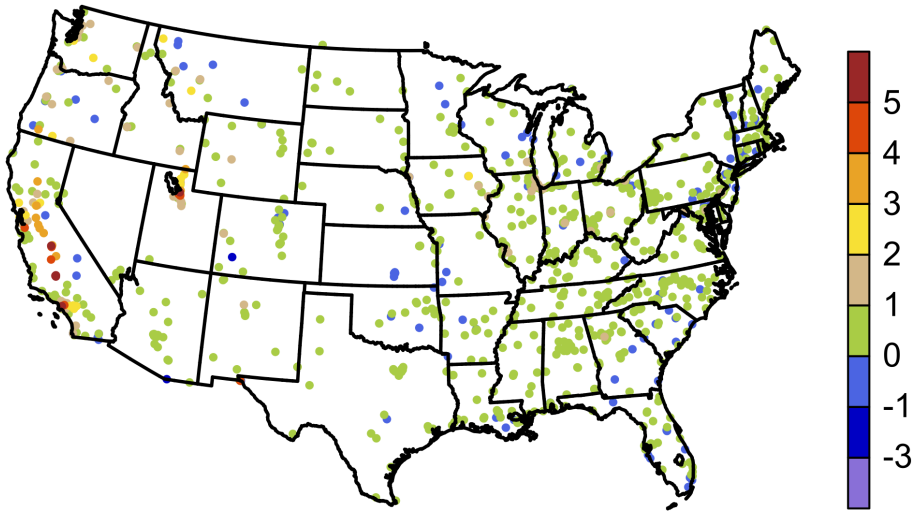

Figure 4. The differences in Standardized Monthly Exceedance Days (SME-days) between PNA+ and PNA− months (PNA+ minus PNA−). The measurements of $PM_{2.5}$ were carried out over 1999–2013, in which there were 18 PNA+ months and 18 PNA− months as shown in Fig. 2a.

ACPD
15, 33209–33251, 2015

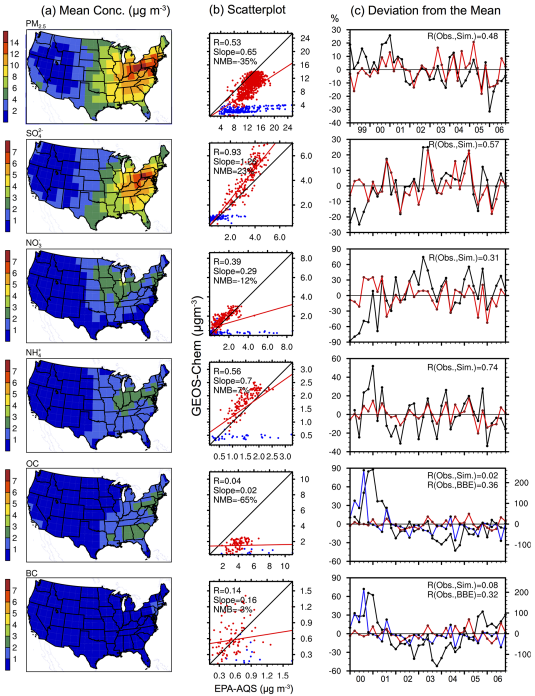

Figure 5. (a) Simulated surface-layer concentrations ($\mu g\,m^{-3}$) of $PM_{2.5}$ (the sum of SO_4^{2-}, NO_3^-, NH_4^+, BC, and OC) and each aerosol species averaged over NDJFM of 1999–2006. **(b)** Scatter plots of the simulated concentrations vs. the EPA-AQS observations. Also shown are the $y = x$ line (black line) and linear fit (red line). The blue and red dots represent sites in the western and eastern US, respectively. **(c)** Comparisons of the deviation from the mean (DM) of observed concentration (black line) with that of simulated concentration (red line) in each winter month for each aerosol species, left axis. Also shown in the panel for OC (BC) the monthly variations in DMof biomass burning emission of OC (BC), blue line, right axis.

ACPD
15, 33209–33251, 2015

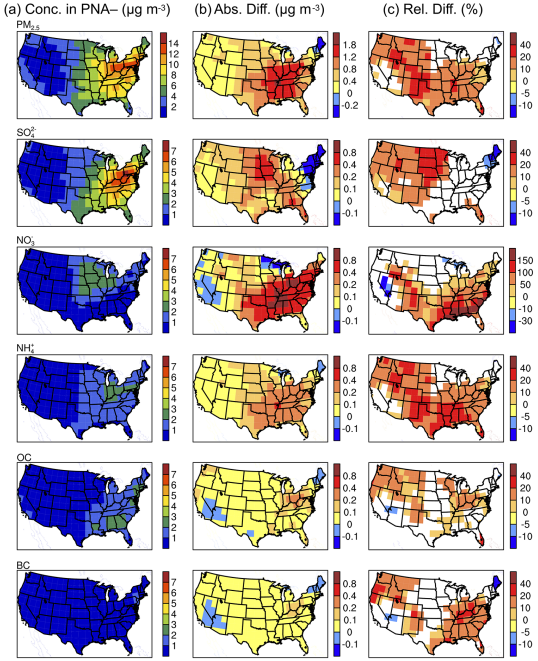

Figure 6. (a) Simulated concentrations ($\mu g\,m^{-3}$) of $PM_{2.5}$ and each aerosols species averaged over the PNA– months of 1986–2006. **(b)** The absolute differences ($\mu g\,m^{-3}$) in simulated aerosol concentrations between PNA+ and PNA– months (PNA+ minus PNA–). **(c)** The relative differences (%) in simulated aerosol concentrations between PNA+ and PNA– months. The white spaces in **(c)** indicate the areas that did not pass the two-tail Student *t* test with 90 % significance level. The seasonal cycles of simulated aerosol concentrations were removed, similar to the treatment for observations in Fig. 3.

ACPD
15, 33209–33251, 2015

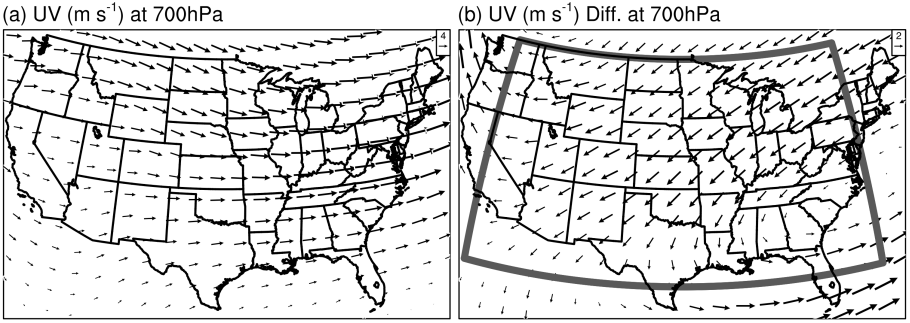

Figure 7. (a) Horizontal winds at 700 hPa averaged over the winter months of NDJFM of 1986–2006, and **(b)** the corresponding differences between the PNA+ and PNA– months. Datasets are from the assimilated GEOS-4 meteorological fields. Also shown in **(b)** is the domain of (75–120° W, 28–49° N) for which transboundary mass fluxes of $PM_{2.5}$ are calculated.

ACPD
15, 33209–33251, 2015

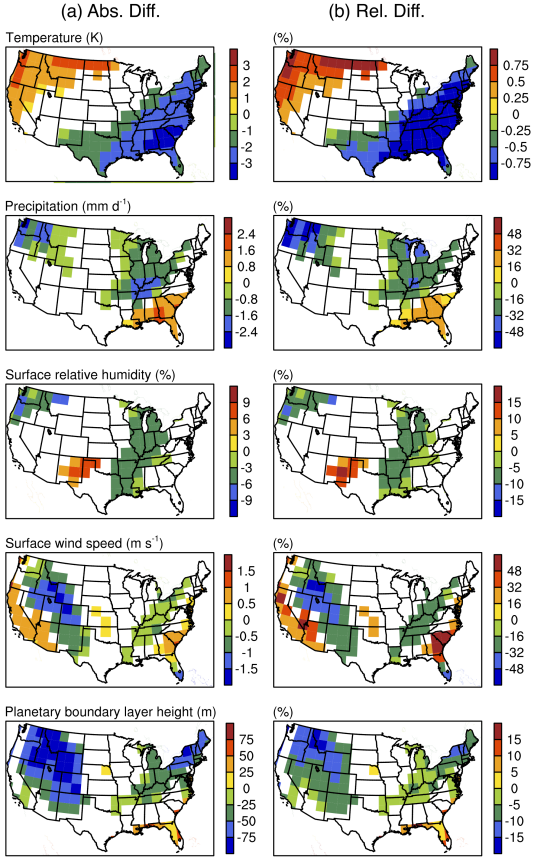

Figure 8. (a) The absolute and **(b)** relative differences in meteorological parameters between PNA+ and PNA− months. Datasets are from the assimilated GEOS-4 meteorological fields. The white spaces in indicate the areas that did not pass the two-tail Student *t* test with 90 % significance level. The seasonal cycles of meteorological variables were removed, similar to the treatment for observations in Fig. 3.

ACPD
15, 33209–33251, 2015